Infrared gas phase study on plasma-polymer interactions in high-current diffuse dielectric barrier discharge

Y. Liu,[1,2] S.Welzel,[1,2] S. A. Starostin,[3] M. C. M. van de Sanden,[1,2] R. Engeln,[2] and H. W. de Vries[1]

[1]*Dutch Institute for Fundamental Energy Research, Eindhoven, 5612 AJ, The Netherlands*

[2]*Eindhoven University of Technology, Eindhoven, 5612 AZ, The Netherlands*

[3]*FUJIFILM Manufacturing Europe B.V., Tilburg, 5047 TK, The Netherlands*

A roll-to-roll high-current diffuse dielectric barrier discharge (DBD) at atmospheric pressure was operated in air and $Ar/N_2/O_2$ gas mixtures. The exhaust gas from the discharge was studied using a high-resolution Fourier-transform infrared (FTIR) spectrometer in the range from 3000 to 750 cm^{-1} to unravel the plasma-polymer interactions. The absorption features of $H_xN_yO_z$, CO_x, and HCOOH (formic acid) were identified, and the relative densities were deduced by fitting the absorption bands of the detected molecules. Strong interactions between plasma and polymer (Polyethylene-2, 6-naphthalate, or PEN) in precursor-free oxygen-containing gas mixtures were observed as evidenced by a high CO_x production. The presence of HCOOH in the gas effluent, formed through plasma-chemical synthesis of CO_x, turns out to be a sensitive indicator for etching. By adding tetraethylorthosilicate (TEOS) precursor in the plasma, dramatic changes in the CO_x production were measured, and two distinct deposition regimes were identified. At high precursor flows a good agreement with the precursor combustion and the CO_x production was observed, whereas at low precursor flows an etching-deposition regime transpires, and the CO_x production is dominated by polymer etching.

I. INTRODUCTION

Atmospheric-pressure dielectric barrier discharge (DBD) is an excellent candidate for plasma enhanced chemical vapor deposition (PECVD) of functional thin films.[1-3] In order to deposit uniform thin films, it is preferable to obtain homogeneous or "glow-like" plasma, which is usually limited to a few noble gases (e.g. helium and argon) under atmospheric pressure.[4-6] In our previous research, a high-current "glow-like" discharge was obtained in air-like gas mixture of $N_2/Ar/O_2$ under atmospheric pressure.[7] The uniformity of the plasma and the high power density make this technology of high applied value in surface treatment as well as in thin film deposition, and excellent SiO_2-like barrier layers on polymeric substrates have been achieved.[3,8,9] Distinct regimes of plasma-polymer interactions along the electrodes were identified with AFM and SEM, and it was concluded that during the film growth process a competition between deposition and etching exists.[10] It is well known that the deposition, or the polymerization process, is very complex as numerous intermediates such as ions and radicals are generated which can interact with the polymer surface.[11] Quantitative measurements of the reactive species on their ground or excited states were carried out by different spectroscopic methods such as optical emission spectroscopy (OES), laser induced fluorescence (LIF) measurement, mass spectroscopy (MS), and

ultraviolet (UV) and infrared (IR) absorption spectroscopy.[12-23] Using an *ex-situ* FTIR, Pipa *et al*. studied the composition of stable molecules from an atmospheric-pressure plasma jet (APPJ) operating in an argon-air mixture.[22] The NO production shows a good agreement with other measurements by emission spectroscopy[24] while additional C-related molecules were attributed to plasma contact with the plastic holder of the APPJ. In this study, a high-current "glow-like" discharge was obtained in an open air roll-to-roll system. Infrared gas-phase studies of the plasma exhaust gas were carried out using a high-resolution FTIR spectrometer. The relative densities of the stable species were deduced according to the fitting of the absorption bands of the detected molecules. By varying the gas composition and the substrate, the mechanisms of the molecule production under etching and deposition conditions were discussed. The purpose of the present study is to obtain a better understanding of the gas phase chemical processes with a particular focus on the plasma-polymer interactions.

II. EXPERIMENTAL SET-UP

The schematic pictures of the roll-to-roll plasma reactor with the gas sampling arrangement and the FTIR absorption measurement system are presented in Figs. 1(a) and (b), respectively. In Fig. 1(a), the discharge was ignited between two curved copper electrodes with a radius of 120 mm and a width of 150 mm, both covered by polymeric substrates (Polyethylene-2, 6-naphthalate, or PEN) of 100 μm thickness as dielectrics. In this study, two types of the dielectric substrates were investigated. One is bare PEN, and another is PEN coated with a 100 nm thick silica layer. The electrode temperature was sustained at 80 ℃ by means of an oil circulation system. The smallest distance between the two electrodes was 0.5 mm. The gas mixture was injected from the left side of the discharge area in Fig. 1(a) while the substrates were transported at 40 mm·min^{-1} in the same direction as the gas flow. The flow rate of the gas mixture was controlled at about 15 slm (standard liter per minute). However, because of the narrow gap (~100 μm) between the gas injector and the electrodes (see Fig. 1(a)), the gas leakage cannot be avoided. This should be taken into account in the calculations involving the gas flow. In this study, the gas loss is estimated at about 30%.[25] In the deposition, the tetraethylorthosilicate (TEOS) precursor was diluted with 1.0 slm argon together with oxygen as the oxidizer and 15 slm nitrogen as the carrier gas. The DBD was powered by a sinusoidal voltage with a frequency of 185 kHz and amplitude up to 2~3 kV. To reduce the power load to the polymer the injected power was modulated at 625 Hz with a duty cycle of 50%. The input power was kept at 600 W with a power density of about 20 W·cm^{-2}. A more detailed description of the experimental set-up can be found elsewhere.[26] The effluent gas from the open air reactor was sampled by 10 pipettes into an IR cell (2.5 L volume, 10 cm inner diameter) downstream of the active plasma phase at about 25 mm distance. The flow rate in the extraction system was set to 2.5 slm with about 2.5 s residence time. To increase sensitivity, the IR cell was equipped with a set of spherical

mirrors and aligned to a total absorption path length of 700 cm at a reduced pressure of 4300 Pa under room temperature (~ 25 °C). The IR cell was directly placed into the sample compartment of the FTIR spectrometer (Bruker, IFS 66/s, ~0.15 cm^{-1} resolution, as shown in Fig. 1(b)). The etching rate of the polymer substrate was determined by measuring a step profile using a white light interferometric microscope (Veeco, Wyko NT9100) in vertical scanning interferometry (VSI) mode. The surface roughness was measured using an AFM (Park, NX10). Moreover, a particle counter (Lighthouse, SOLAIR 1100 PLUS) with 0.1 micron sensitivity was mounted about 20 cm downstream the plasma reactor to detect the particles after the etching.

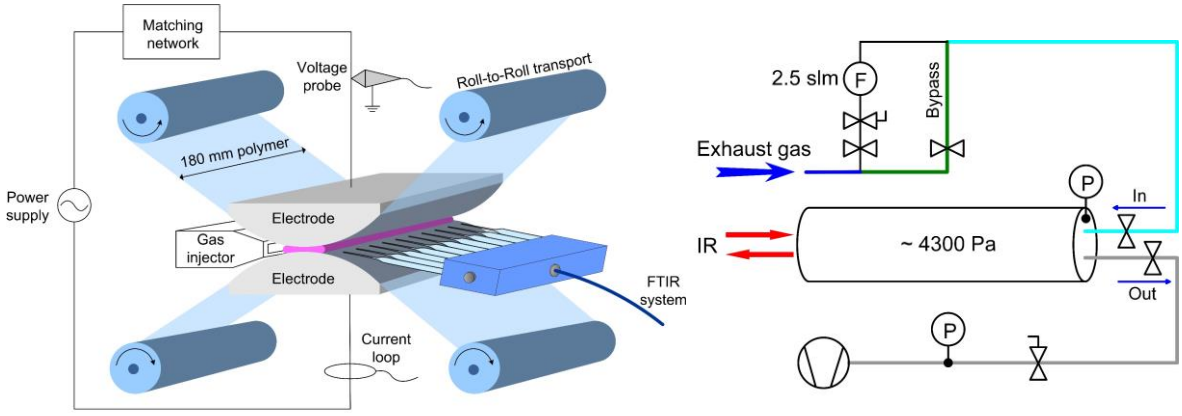

(a) (b)

FIG. 1. Experimental setup to (a) generate plasma and (b) carry out *ex-situ* FTIR absorption spectra measurement.

III. RESULTS AND DISCUSSION

A. Identification of the absorption spectra

A typical infrared spectrum of the atmospheric-pressure air (15 slm) plasma with bare PEN substrate is presented in Fig. 2. In the range of 3000 to 750 cm^{-1}, only H_2O and CO_2 were detected in the absorption spectrum of the background air. When the plasma was switched on, both N-related species (HNO_2, N_2O, NO_2, NO) and C-related species (HCOOH, CO, CO_2) could be clearly identified. Ozone, which is frequently observed in air-containing DBDs,[27-30] was not detected under our experimental conditions. The OH radical, detected from OES, was absent here due to its high reactivity, short lifetime and therefore low density.[22]

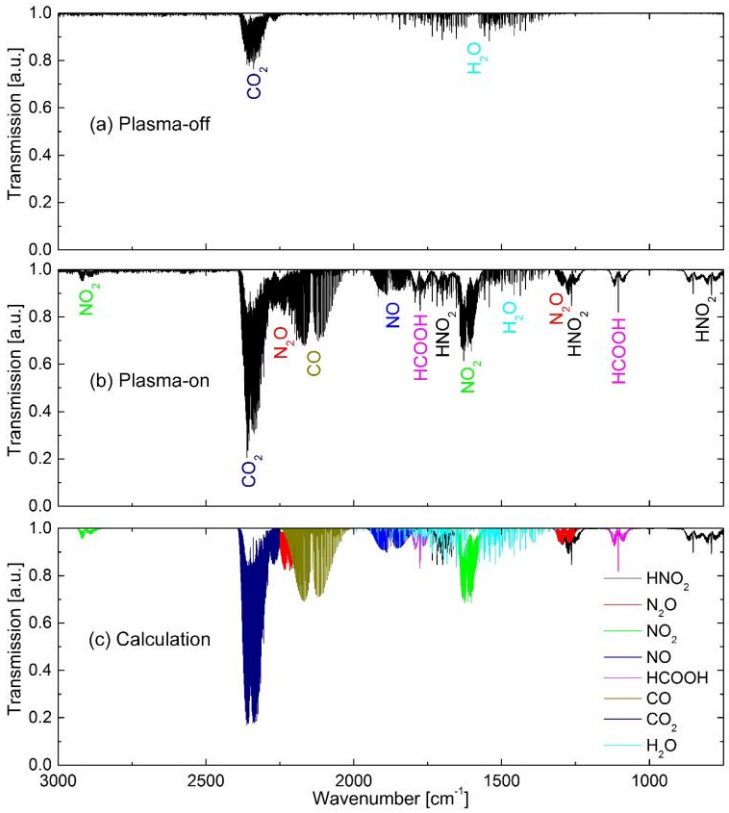

FIG. 2. Identification of stable reaction products in air plasmas with bare PEN substrate: Transmission spectra in the case of (a) plasma off, (b) plasma on and (c) the calculated spectrum.

To acquire quantitative information of the detected molecules from the absorption spectra, the transmission spectra of the molecules except HNO_2 were calculated according to the spectral line parameters given in the HITRAN database using Q-MACSoft-HT software.[31] The HNO_2 spectral line parameters are not available in the HITRAN database. The transmission spectrum of HNO_2 was calculated based on values for the cross section from the Pacific Northwest National Laboratory Northwest IR (PNNL-NWIR) database[32] and by convolving the result with the instrumental broadening. To simplify the data processing, a Gaussian profile with a full width at the half maximum (FWHM) of about 0.15 cm^{-1} was assumed for the instrumental broadening. The relative density η (number of molecules to the total amount of species, ppm) of the detected molecules were estimated by (manually) comparing the calculated transmission spectra with the measured ones. It is clear that this approach is limited to the small molecules with well-resolved ro-vibrational features. The molecules that were analyzed in this way in conjunction with the spectral range used for the calculation and with their limit of detection for the experimental conditions given above are summarized in Table. 1. The detection limit for most molecular species (relative density) is of the order of 10 ppm which corresponds to 10^{14} cm^{-3} at atmospheric pressure. These values are based on a signal-to-noise ratio of 1. Typical noise values are 0.5 to 1.5 × 10^{-3} in the transmission spectra. Usually the error level is a

few times higher than the limit of detection. Besides, the overlapping of the spectral lines e.g. CO, N_2O and CO_2 in the range from 2300 to 2150 cm^{-1} also induces errors in the molecule density estimation.

Table. 1 Summary of molecules observed and quantified via spectral line data

Molecule	**Spectral range [cm^{-1}]**	**Limit of detection [ppm]**
HNO_2	1659, 1274	20
N_2O	2255-2185	5
NO_2	1612-1590	5
NO	1925-1845	20
HCOOH	1810-1750	10
CO	2230-2030	10
CO_2	2270-2260	100

B. Air and Air-Ar plasma

For thin film deposition, the plasma is operated in an air-like gas mixture with addition of Ar as the precursor carrier gas. Because the role of Ar in the gas phase chemistry of the plasma is not known, the relative densities were measured in air (15 slm) and air/Ar (15 slm / 1.0 slm) gas mixture with bare PEN substrate. The electrical characteristics are very similar and stable with a single smooth current pulse which indicates a diffuse discharge under both conditions.[33] The corresponding relative densities are shown in Fig. 3. Both N-related and C-related species are not significantly changed with the addition of Ar and can be characterized by $\eta(HNO_2) < \eta(N_2O) < \eta(NO_2) < \eta(NO)$ and $\eta(HCOOH) < \eta(CO) < \eta(CO_2)$, respectively. This analysis suggests that addition of Ar is not required to sustain the discharge, and Ar can be used for admixing the precursor without significantly influencing the plasma chemistry.

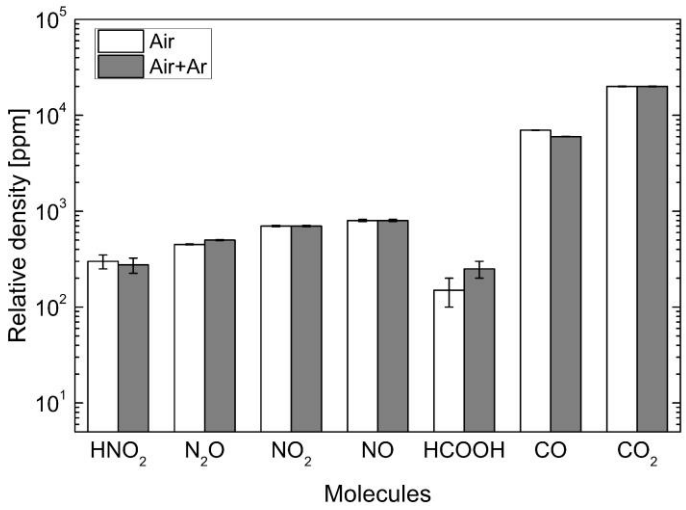

FIG. 3. Relative densities of stable molecules in a) air (15 slm) and b) air/Ar (15 slm / 1.0 slm) gas mixture with bare PEN substrate.

C. Effect of oxygen concentration

The absorption spectra of Ar/N_2 (1.0 slm / 15 slm) and $Ar/N_2/O_2$ (1.0 slm / 15 slm / 2.0 slm) gas mixtures with bare PEN substrate are shown in Fig. 4(a). In Ar/N_2 (1.0 slm / 15 slm) gas mixture, only CO and CO_2 were detected in the spectrum, and the relative densities of 1500 ppm and 1000 ppm were estimated, respectively. As soon as O_2 (2.0 slm) was injected, $\eta(CO)$ and $\eta(CO_2)$ increase to 4800 ppm and 10000 ppm as well as that HCOOH and N-related species (HNO_2, N_2O, NO_2 and NO) appear in the spectrum. The variations of the molecule relative densities with respect to oxygen relative density in $Ar/N_2/O_2$ (1.0 slm / 15 slm / 0.5~2.0 slm) gas mixture with bare PEN substrate were estimated, as shown in Fig. 4(b). All N-related products and HCOOH clearly increase with the O_2 content in the gas flow while $\eta(CO)$ and $\eta(CO_2)$ remain relatively stable at about 1 order higher level than the N-related species. Typically, the relative densities for the latter species are all in the order of 100 ppm. With an extrapolation of the increasing trends in Fig. 4(b) to an O_2 flow of about 4.0 slm (i.e. 20% in the mixture as in case of air), the relative densities of $\eta(HNO_2)$, $\eta(N_2O)$, $\eta(NO_2)$ and $\eta(NO)$ would be ~ 200 ppm, ~ 300 ppm, ~ 500 ppm and ~ 800 ppm, respectively. These extrapolated results are indeed close to the ones observed experimentally for air/Ar (15 slm / 1.0 slm) plasmas in contact with bare PEN substrate (Fig. 3, $\eta(HNO_2)$ ~ 250 ppm, $\eta(N_2O)$ ~ 450 ppm, $\eta(NO_2)$ ~ 650 ppm and $\eta(NO)$ ~ 800 ppm).

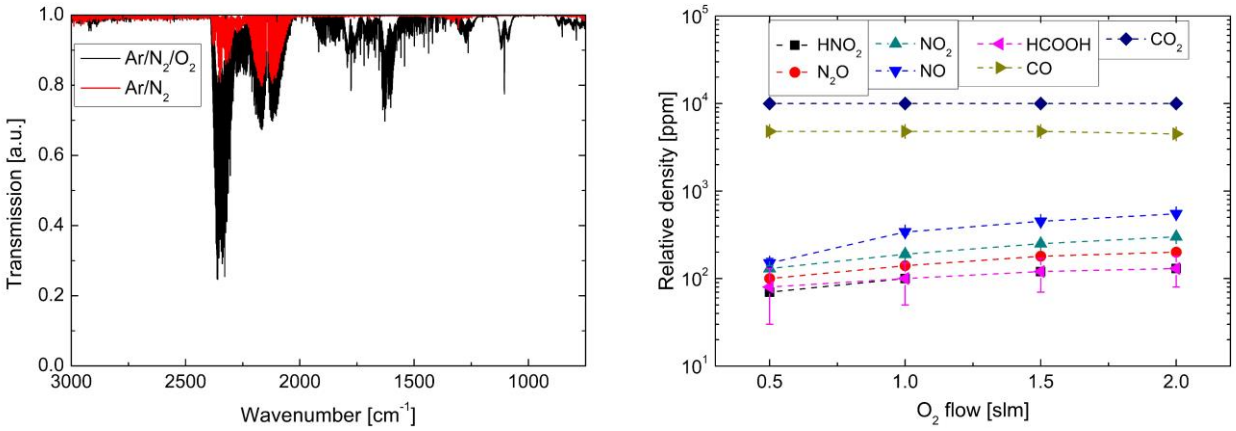

(a) (b)

FIG. 4. (a) Comparison of absorption spectra in Ar/N_2 (1.0 slm / 15 slm) and $Ar/N_2/O_2$ (1.0 slm / 15 slm / 2.0 slm) gas mixtures and (b) variations of the relative densities of stable molecules in $Ar/N_2/O_2$ (1.0 slm / 15 slm / 0.5~2.0 slm) plasmas in contact with bare PEN substrate.

D. N-related reactions

The relative densities of the main gas phase components in $Ar/N_2/O_2$ (1.0 slm / 15 slm / 2.0 slm) plasmas in contact with substrates of bare PEN and PEN covered by 100 nm silica layer are shown in Fig. 5. Both the N-containing and the C-containing productions vary significantly under the two conditions.

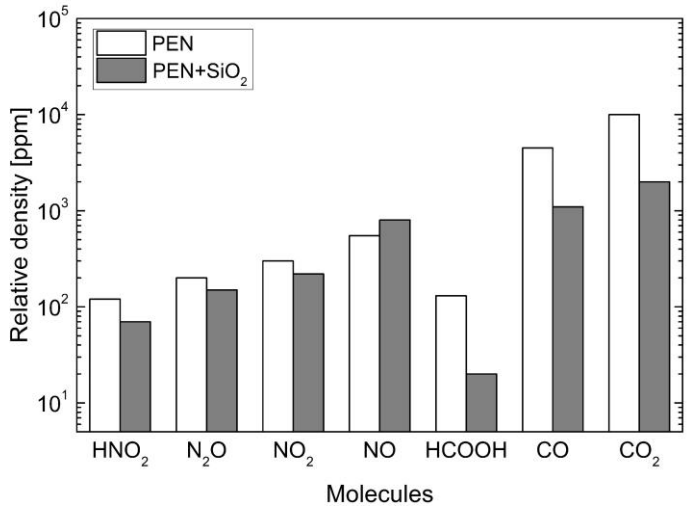

FIG. 5. Relative densities in $Ar/N_2/O_2$ (1.0 slm / 15 slm / 2.0 slm) plasmas in contact with substrates of bare PEN and silica coated PEN foil.

It is well known that the plasma-surface interactions (e.g. etching and deposition) are closely related to the reactive species (e.g. O, O_3, OH and HO_2) which, in this study, can be reflected by the information of N-related molecules. Therefore it is important to study the reactions between the $H_xN_yO_z$ molecules.

The dominant reaction pathways for plasma remediation of $H_xN_yO_z$ molecules are shown in Fig. 6. Here the reaction scheme is simplified from Ref. 34 based on the infrared active molecules that are identified in the absorption spectra. These molecules are shown in bold in Fig. 6. In the reaction pathways, NO, which can be regarded as the initial specie, is mainly generated through the reactions between N and oxygen containing species (O_2, OH), as labelled as reaction (1). Then NO can be remediated through either reduction with N and generating N_2 [reaction (2)], or oxidation with O, O_3 or HO_2 and generating NO_2 [reactions (3), (4) and (5)]. HNO_2, which is generated from the oxidation between NO and OH [reaction (6)], can be further oxidized into NO_2 with enough OH, reaction (7). NO_2 can also be reduced with N to produce NO through reaction (8)) or N_2O through reaction (9).

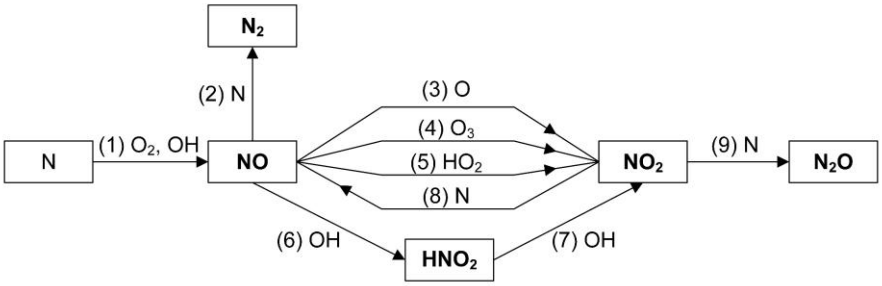

FIG. 6. Schematic of the dominant reaction pathways for plasma remediation of $H_xN_yO_z$.

In Fig. 5, the relative densities $\eta(HNO_2)$, $\eta(N_2O)$, $\eta(NO_2)$ and $\eta(NO)$ with SiO_2-coated PEN are about 110 ppm, 280 ppm, 400 ppm and 1100 ppm, respectively. As soon as the polymer is exposed to the plasma, $\eta(NO)$ decreases to 800 ppm while $\eta(HNO_2)$, $\eta(N_2O)$ and $\eta(NO_2)$ increase to about 275 ppm, 460 ppm and 680 ppm. This indicates that the $H_xN_yO_z$ plasma chemistry is influenced by the plasma-polymer interactions. When these interactions occur, the reaction pathways [Fig. 6] are shifted in the direction from NO to NO_2 due to enhanced oxidization. The increase of HNO_2 with bare PEN further indicates that, OH, which contributes to the generation of HNO_2 [reaction (6)], can be produced from reactions with the polymer.

As mentioned before, ozone is absent in the absorption spectrum. It is very likely 'poisoned' as e.g. described in Ref. 1 [reaction (4)] which is supported by the observed levels of NO/NO_2 and the absence of N_2O_5 in the absorption spectrum.

Moreover, the ozone generation efficiency decreases drastically under the condition of a high electric field or a high gas temperature.[35] This is in accordance with earlier characterization of the high power density (10-20 $W \cdot cm^{-2}$) plasma when the effective reduced electric field strength (E/N) and the gas temperature of the air-like DBD were estimated to be about 150 Td[36] and 200-300 ^{o}C,[37] respectively.

E. C-related reactions

1. CO, CO_2 vs HCOOH

CO and CO_2 are well known precursor molecules for the formation of HCOOH in the gas phase in plasma-chemical processes. The HCOOH formation is explained by Ref. 38 through the plasma-chemical synthesis of high initially oxidized mixtures (CO-H_2O or CO_2-H_2):

$$CO + H_2O \rightarrow HCOOH, \quad (3\text{-}1)$$

$$CO_2 + H_2 \rightarrow HCOOH. \quad (3\text{-}2)$$

Under different conditions, e.g. in oxygen-free or oxygen-containing gas mixtures with bare or silica-coated PEN, we observed a correlation between η(HCOOH) and $\eta(CO_x)$. In Fig. 7, the correlation of the relative densities of CO_x are shown as a function of η(HCOOH). Here η(HCOOH) is not controlled but summarized from all the data obtained under different conditions. The production of HCOOH is closely related to those of CO and CO_2, and an approximately linear fit of $\eta(CO_2)$ and η(CO) is obtained with η(HCOOH). $\eta(CO_2)$ is about 100 times higher, and η(CO) is about 30 times higher than η(HCOOH). Moreover, the CO_x production with bare PEN is much higher than with SiO_2 coated PEN, and η(HCOOH) does not exceed 50 ppm in the case of SiO_2 coated PEN. The mechanism of the carbon-related molecule production will be discussed in the next section.

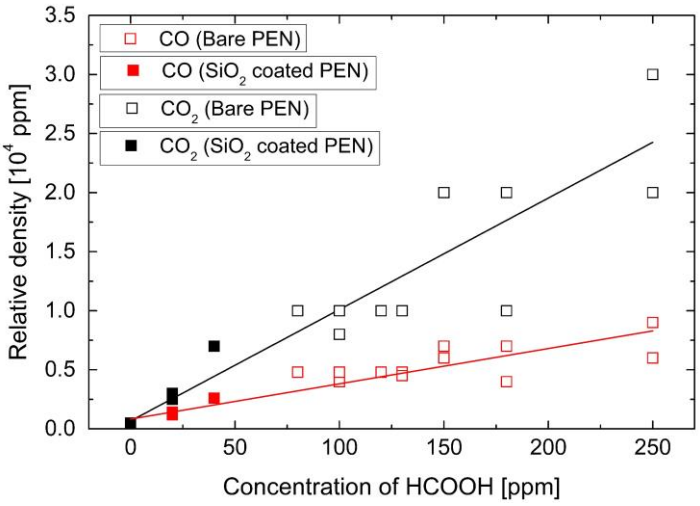

FIG. 7. Variations of $\eta(CO_x)$ with η(HCOOH) in different gas mixtures and substrates. The open symbols represent the relative densities of carbon products formed after plasma exposure with bare PEN while the solid symbols represent plasma exposure of SiO_2 coated PEN. Note, the HCOOH production is not controlled but summarized from the results under the different conditions.

2. Carbon sources

To identify the possible carbon sources, the relative densities of CO and CO_2 were measured for different plasma conditions: with and without oxygen addition, with bare PEN and SiO_2 coated PEN, as presented in Fig. 8.

In the oxygen-free gas mixtures (Ar/N_2 (1.0 slm / 15 slm)), only a small amount of CO_x is observed both in the case of bare PEN and SiO_2-coated PEN. The CO_x production is mainly related to the reactions between oxygen from the ambient air and carbon impurities in the experimental system. These background impurities are inevitable under the current conditions and contribute for about 200-300 ppm to the total production of CO_x. The small amount of oxygen results in an oxygen deficient chemistry and consequently a higher production of CO than CO_2.

In the oxygen-containing gas mixtures ($Ar/N_2/O_2$ (1.0 slm / 15 slm / 2.0 slm)) with SiO_2 coated PEN, the production of CO_x is mainly related to the reactions between the reactive species from the plasma and carbon impurities in the experimental system e.g. the plastic holders and tubes. Similar carbon impurities were also observed in an APPJ system operating in Ar with 0.1% air.[22] Moreover, it should be realized that in the present experimental set-up, deposition experiments were operated prior to the current measurements. The organic precursor molecules absorbed on the walls of the experimental system can be desorbed and oxidized in subsequent experiments and therefore contribute to the CO_x production. Since a high relative density of oxygen is present, the carbon impurities in the system can be more intensively oxidized resulting in a higher $\eta(CO_2)$ (about 2000 ppm) than η(CO) (about 1100 ppm).

In the $Ar/N_2/O_2$ (1.0 slm / 15 slm / 2.0 slm) gas mixture with bare PEN, $\eta(CO)$ and $\eta(CO_2)$ increase drastically to about 4500 ppm and 10000 ppm, respectively. As discussed, the oxidation of the background carbon impurities contributes over 3000 ppm to the total CO_x production. The extra ~11000 ppm of CO_x is therefore due to the interactions between the $Ar/N_2/O_2$ plasma and the PEN substrate.

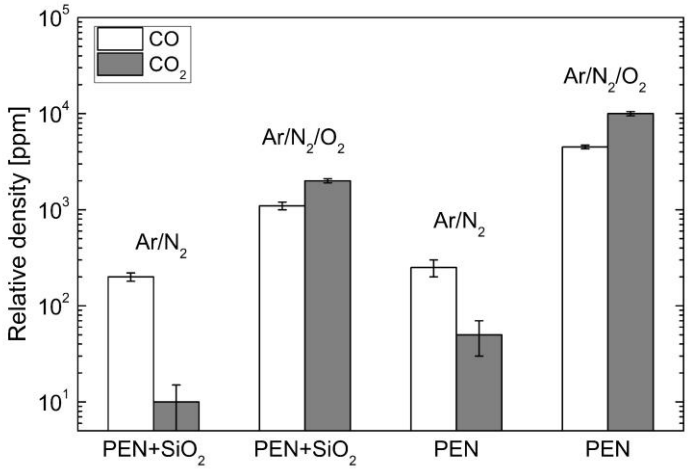

FIG. 8. Relative densities of CO and CO_2 under different experimental conditions in Ar/N_2 (1.0 slm / 15 slm) and $Ar/N_2/O_2$ (1.0 slm / 15 slm / 2.0 slm) gas mixtures with bare PEN or SiO_2-coated PEN.

3. Surface etching

It is known that bare PEN can be etched when exposed to an oxygen containing plasma.[39] To determine the etching rate, the PEN was partly protected by tape and exposed to the air plasma region (with a width of ~15 mm) at a substrate transport speed of 40 mm·min^{-1} equivalent to about 22.5 s exposure time in the plasma. After the plasma treatment the tape was removed, and the height difference of the step profile was determined using an interferometer in vertical scanning interferometry (VSI) mode, as presented in Fig. 9. In addition the surface roughness of pristine and etched PEN was measured using AFM, as shown in Fig. 10.

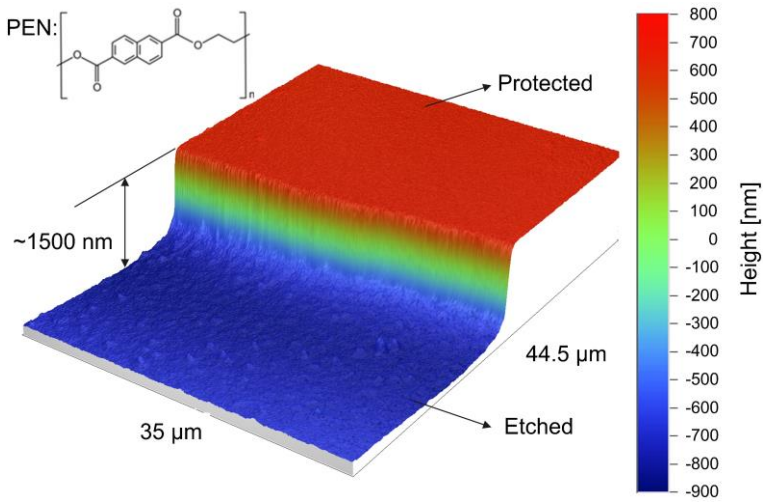

FIG. 9. Interferometric microscopy of air plasma treated PEN in the area near the etching edge.

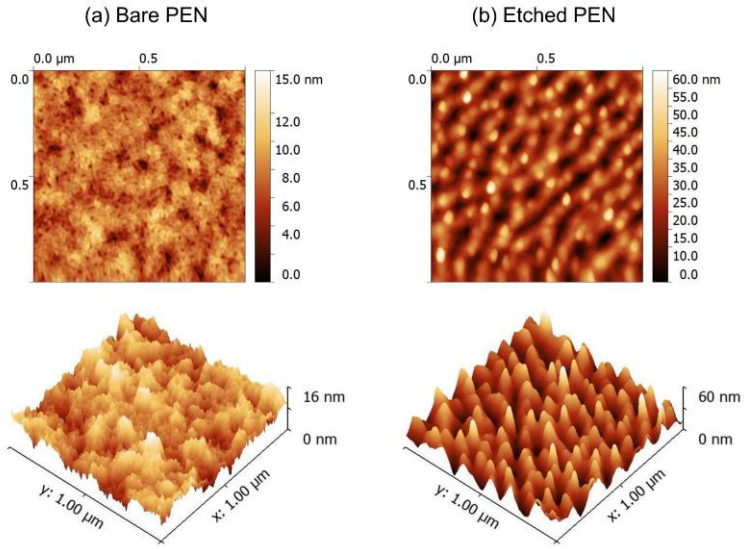

FIG. 10 AFM scan images of (a) bare PEN with the semi-crystalline morphology and (b) etched PEN.

After the plasma treatment, the surface RMS (root mean square) roughness of the PEN increases from ~ 1.5 nm to ~ 5 nm, see Fig. 10. The height difference of the step is ~ 1500 nm which results in an etching rate of ~ 67 nm·s^{-1}. From the amount of the etched PEN, the mass production rate Δm(PEN) of the polymer can be estimated:

$$\Delta m(\mathrm{PEN}) = \Delta V(\mathrm{PEN}) \times \rho(\mathrm{PEN}) = 2 \times \Delta d(\mathrm{PEN}) \times l \times v \times \rho(\mathrm{PEN}) = 4.1 \times 10^{-4}\ \mathrm{g \cdot s^{-1}}, \quad (3\text{-}3)$$

where ΔV(PEN) is the etched volume production of PEN substrate per second, ρ(PEN) is the density of PEN (1.36 g·cm^{-3}), Δd(PEN) is the thickness of the etched PEN (~ 1500 nm), l is the substrate width (150 mm), and v is the transport velocity of the PEN substrate (40 mm·min^{-1}).

The molecule production rate of carbon ΔX(C) can be estimated as:

$$\Delta X(\mathrm{C}) = \frac{168}{242} \times \Delta m(\mathrm{PEN}) \times \frac{N_A}{M(\mathrm{C})} = 1.4 \times 10^{19}\ \mathrm{molecules \cdot s^{-1}}, \quad (3\text{-}4)$$

where N_A is the Avogadro's number (6.02×10^{23} mol^{-1}), and M(C) is the molar mass of carbon (12 g·mol^{-1}).

Assuming all the carbon from the etched PEN is fully oxidized and converted to CO_x, the relative density $\eta(CO_x)$ is:

$$\eta(\mathrm{CO_x}) = \frac{\Delta X(\mathrm{CO_x})}{\Delta X(\mathrm{gas\ flow})} = \frac{\Delta X(\mathrm{CO_x}) \times V_\mathrm{m}}{\Delta \Phi(\mathrm{gas\ flow}) \times N_\mathrm{A}} \sim 3300\ \mathrm{ppm}, \quad (3\text{-}5)$$

where $\Delta X(CO_x)$ is the molecule production rate of CO_x (1.15×10^{19} molecules·s^{-1}), ΔX(gas flow) is the molecule flow rate, $\Delta \Phi$(gas flow) is gas flow rate (15×0.7 slm considering a 30% gas leakage) and V_m is the molar volume (24.5 L·mol^{-1} at 25 ℃).

In Sec. III E 2, we measured $\eta(CO_x)$ of about 14500 ppm in Ar/N_2/O_2 (1.0 slm / 15 slm / 2.0 slm) plasma with bare PEN substrate. Among the total CO_x production, more than 3000 ppm is attributed to the oxidization of the background carbon impurities, and the extra 11000 ppm CO_x is due to the plasma-polymer interactions. The calculated value of CO_x from PEN etching (~3300 ppm) is about 3 times lower than the measured value (~11000 ppm). However, the etching should still be the main factor that contributes to the high value of CO_x production. In the above calculation, we assumed that all the carbon from the etched PEN is fully oxidized and converted to CO_x. In order to verify this assumption the exhaust gas was probed by a particle counter during the etching process of bare PEN. A large amount of sub-micron sized particles are detected during exposure of the bare PEN, as presented in Fig. 11. According to Liston *et al.*[39] etching of the polymer material can take place. Moreover, the etching rate of semi-crystalline polymers such as PEN is preferential i.e. the amorphous regions have higher

etch rate than the crystalline regions, see Fig. 10b. This suggests that in the etching process small (less than 10 nm) partially oxidized polymer fragments are produced and agglomerate during transport in the gas flow forming bigger particles (> 100 nm).[40] The initially airborne particles may attach on the inner surface of the FTIR system (memory effect) and further decompose into CO_x species and thus artificially enhance the FTIR absorption signal. However, not much is known in the polymer interactions with the oxygen-containing plasma.[41] Further studies and more systematic measurements are required to support this hypothesis.

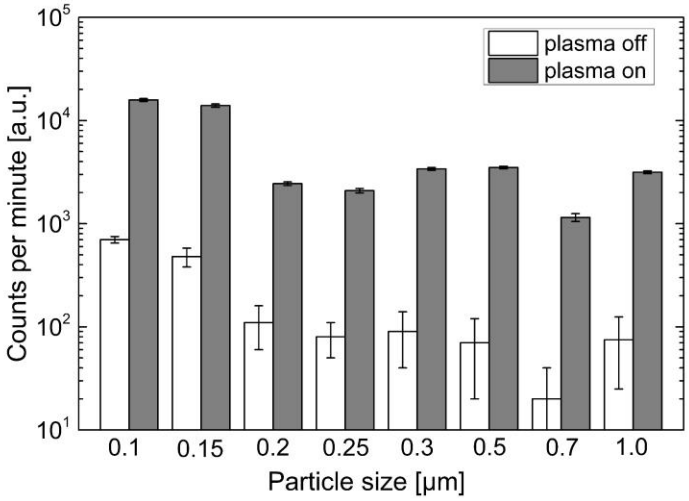

FIG. 11. Particle counts of the exhaust gas during the air-like plasma exposure with bare PEN.

4. Deposition

In addition, the carbon balance was studied under deposition conditions. The relative densities of CO_x were measured with respect to the amount of TEOS added in an $Ar/N_2/O_2$ (1.0 slm / 15 slm / 0.8 slm) gas mixture. The results of the measurements are shown in Fig. 12. The trends of the measured $\eta(CO_x)$ with TEOS injection can be divided into two regimes. In regime (1) a strong decrease of $\eta(CO_x)$ with the addition of a small amount of TEOS (less than 150 ppm) is observed whereas in regime (2) a clear increase of the $\eta(COx)$ with increasing TEOS flow (more than 150 ppm) is obtained. This indicates different mechanisms of CO_x production. Moreover, the calculated values of $\eta(CO_x)$ are approximately the same as the measured ones in regime (2). Hence, the CO_x production in regime (2) can be attributed to the full combustion of the precursor.

As concluded in Ref. 10, the etching and deposition can be competing mechanisms in thin film growth. In regime (2) where the amount of TEOS is relatively high, the etching is weak and the surface of PEN is quickly covered by a SiO_2 layer.

However, in regime (1) the plasma surface reactions are much more complicated. Since the amount of TEOS is relatively low, the surface of PEN is not completely covered by silica layer during the early exposure of the substrate to the plasma region. Oxygen radicals have more time to interact with the polymer surface leading to simultaneous etching and deposition during the film growth process. As discussed in Sec. III E 3, the polymer etching and the generation of a large amount of particles can significantly influence the measurement of $\eta(CO_x)$ in the FTIR system. Consequently, the CO_x production in regime (1) is dominated by etching which results in overrated values of $\eta(CO_x)$, as presented in Fig. 12.

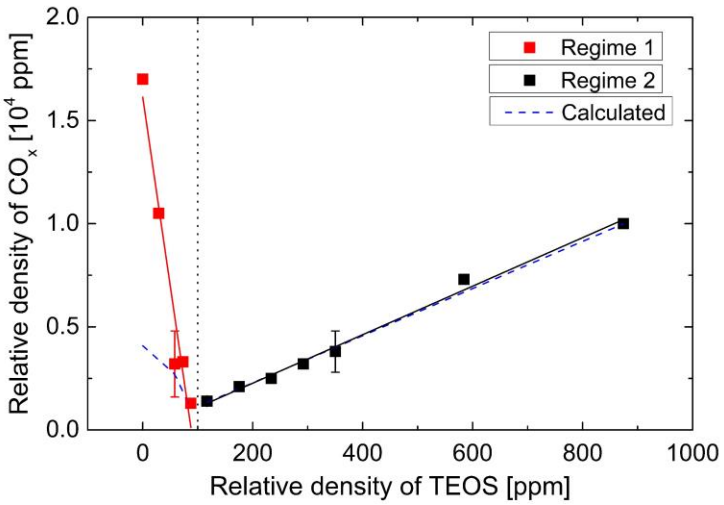

FIG. 12. Comparison of measured $\eta(CO_x)$ in $Ar/N_2/O_2$ (1.0 slm / 15 slm / 0.8 slm) plasma with 0-875 ppm TEOS in contact with bare PEN with calculated $\eta(CO_x)$ from the fully dissociation of etched particles and precursor molecules.

IV. CONCLUSIONS

In this study, the Fourier transform infrared (FTIR) gas-phase analysis of stable molecules in the gas effluent of the atmospheric-pressure plasmas was reported. The absorption features of the plasma species were analyzed. Both N-related species (HNO_2, N_2O, NO_2, NO) and C-related species (HCOOH, CO, CO_2) were identified, and the corresponding relative densities were estimated according to the calculations based on the line parameters given in the HITRAN and PNNL databases. The N-related species were characterized by $\eta(HNO_2) < \eta(N_2O) < \eta(NO_2) < \eta(NO)$ and reflect the information of the reactive species (e.g. O, O_3, OH and HO_2) in the plasma. In the case of bare PEN the reaction pathways of $H_xN_yO_z$ were shifted in the direction from NO to NO_2 due to enhanced oxidation reactions.

The measurement of high rates of CO_x species indicates strong interactions between the oxygen-containing plasma and the polymer (as is produced due to etching of PEN). Formic acid (HCOOH) is identified as a sensitive indicator for plasma-polymer

interactions. The sources of CO_x are discussed in relation to oxidation of the background carbon pollution which contributes about 3000 ppm, whereas the etching of the bare PEN substrate contributes about 11000 ppm to the CO_x relative density. The estimated values of CO_x cannot be totally explained on the basis of the amount of polymer removed by etching. It is argued that partially oxidized airborne particles are produced during etching that accumulate in the low pressure FTIR cell and subsequently decompose and release CO_x species. By adding precursor (TEOS) in the plasma two different regimes were identified. At increased precursor flows (above 150 ppm) the production of CO_x is dominated by precursor dissociation and a linear increase of the CO_x species can be directly correlated with the amount of carbon from the precursor combustion. At much lower precursor flows (less than 150 ppm), an etching-deposition regime transpires and etching becomes an increasingly dominant factor in the process.

ACKNOWLEDGMENTS

This work was supported by the EOS-KT project and the Industrial Partnership Programme i31 (APFF) that is carried out under an agreement between FUJIFILM Manufacturing Europe B.V. and FOM, which is part of the Netherlands Organization for Scientific Research (NWO).

REFERENCES

[1]U. Kogelschatz, Plasma Chem. Plasma Process. **23**, 1-46 (2003).

[2]F. Massines, C. Sarra-Bournet, F. Fanelli, N. Naude, and N. Gherardi, Plasma Process. Polym. **9**, 1041-1073 (2012).

[3]S. A. Starostin, M. Creatore, J. B. Bouwstra, M. C. M. van de Sanden, and H. W. de Vries, Plasma Process. Polym. **12**, 545-554 (2014).

[4]S. Kanazawa, M. Kogoma, T. Moriwaki, and S. Okazaki, J. Phys.D: Appl. Phys. **21**, 838-840 (1988).

[5]S. Okazaki , M. Kogoma, and H. Uchiyama, in *Proceedings of the 3rd International Symposium on High Pressure Low Temperature Plasma Chemistry (HAKONE III)*, Strasbourg, France, September (1991), Vol. 101, pp. 3–5.

[6]S. Okazaki, M. Kogoma, M. Uehara, and Y. Kimura, J. Phys.D: Appl. Phys. **26**, 889-892 (1993).

[7]S. A. Starostin, M. A. M. ElSabbagh, E. Aldea, H. W. de Vries, M. Creatore, and M. C. M. van de Sanden, IEEE Trans. Plasma Sci. **36**, 968-969 (2008).

[8]P. A. Premkumar, S. A. Starostin, M. Creatore, H. W. de Vries, R. M. J. Paffen, P. M. Koenraad, and M. C. M. van de Sanden, Plasma Process. Polym. **7**, 635-639 (2010).

[9]S. A. Starostin, P. A. Premkumar, M. Creatore, H. W. de Vries, R. M. J. Paffen, and M. C. M. van de Sanden, Appl. Phys. Lett. **96**, 061502 (2010).

[10]P. A. Premkumar, S. A. Starostin, H. W. de Vries, M. Creatore, R. M. J. Paffen, T. J. Eijkemans, P. M. Koenraad, and M. C. M. van de Sanden, Plasma Process. Polym. **6**, 693-702 (2009).

[11]H. Yasuda, J. Polym. Sci., Macromol. Rev. **16**, 199-293 (1981).

[12]R. Brandenburg, J. Ehlbeck, M. Stieber, T. V. Woedtke, J. Zeymer, O. Schluter, and K. -D. Weltmann, Contrib. Plasma Phys. **47**, 72-79 (2007).

[13]V. Schulz-von der Gathen, L. Schaper, N. Knake, S. Reuter, K. Niemi, T. Gans, and J. Winter, J. Phys.D: Appl. Phys. **41**, 194004 (2008).

[14]R. Ono, and T. Oda, IEEE Trans. Ind. Appl. **37**, 709-714 (2001).

[15]G. Dilecce, P. F. Ambrico, M. Simek, and S. de Benedictis, Chem. Phys. **398**, 142-147 (2012).

[16]H. Singh, J. W. Coburn, and D. B. Graves, J. Vac. Sci. Technol. A **17**, 2447-2455 (1999).

[17]H. Singh, J. W. Coburn, and D. B. Graves, J. Vac. Sci. Technol. A **18**, 299-305 (2000).

[18]S. Agarwal, G. W. W. Quax, M. C. M. van de Sanden, D. Maroudas, and E. S. Aydil, J. Vac. Sci. Technol. A **22**, 71-81 (2004).

[19]F. Fanelli, S. Lovascio, R. d'Agostino, F. Arefi-Khonsari, and F. Fracassi, Plasma Process. Polym. **7**, 535-543 (2010).

[20]F. Fanelli, R. d'Agostino, and F. Fracassi, Plasma Process. Polym. **8**, 932-941 (2011).

[21]J. -P. Booth, G. Cunge, F. Neuilly, and N. Sadeghi, Plasma Sources Sci. Technol. **7**, 423-430 (1998).

[22]A. V. Pipa, and J. Röpcke, IEEE Trans. Plasma Sci. **37**, 1000-1003 (2009).

[23]S. Reuter, J. S. Sousa, G. D. Stancu, and J-P. H. van Helden, Plasma Sources Sci. Technol. **24**, 054001 (2015).

[24]A. V. Pipa, T. Bindemann, and K. -D. Weltmann, in *International Conference on Phenomena in Ionized Gases (ICPIG)*, Prague, Czech Republic, 15-20 July 2007, pp.06-25.

[25]S. A. Starostin, M. Creatore, J. B. Bouwstra, M. C. M. van de Sanden and H. W. de Vries, Plasma Process. Polym. **12**, 545-554 (2015).

[26]S. A. Starostin, E. Aldea, H. W. de Vries, M. Creatore and M. C. M. van de Sanden, Plasma Process. Polym. **4**, S440-S444 (2007).

[27]S. Yagi, and M. Tanaka, J. Phys. D: Appl. Phys. **12**, 1509-1520 (1979).

[28]U. Kogelschatz, B. Eliasson, and M. Hirt, Ozone Sci. Eng. **10**, 367-378 (1988).

[29]N. Osawa, H. Kaga, Y. Fukuda, S. Harada, Y. Yoshioka, and R. Hanaoka, Eur. Phys. J. Appl. Phys. **55**, 13802 (2011).

[30]A. Deryugin, A. Napartovich, C. Gorse, F. Paniccia, and M. Capitelli, Plasma Chem. Plasma Process. **17**, 79-91 (1997).

[31]L. S. Rothman, and et al., J. Quant. Spectrosc. Ra. **110**, 533-572 (2009).

[32]S. W. Sharpe, T. J. Johnson, R. L. Sams, P. M. Chu, G. C. Rhoderick, and P. A. Johnson, Appl. Spectrosc. **58**, 1452-1461 (2004).

[33]S. A. Starostin, S. Welzel, Y. Liu, B. van Velden-Schuermans, J. B. Bouwstra, M. C. M. van de Sanden, and H. W. de Vries, Eur. Phys. J. Appl. Phys. **71**, 20803 (2015).

[34]A. C. Gentile, Ph.D. thesis, Urbana-Champaign, 1995.

[35]J. Kitayama, and M. Kuzumoto, J. Phys. D: Appl. Phys. **32**, 3032-3040 (1999).

[36]B. M. Penetrante, M. C. Hsiao, B. T. Merritt, G. E. Vogtlin, P. H. Wallman, M. Neiger, O. Wolf, T. Hammer, and S. Broer, Appl. Phys. Lett. **68**, 3719-3721 (1996).

[37]S. A. Starostin, S. Welzel, M. C. M. van de Sanden, J. B. Bouwstra, and H. W. de Vries, in *XXII Europhysics Conference on Atomic and Molecular Physics of Ionized Gases (ESCAMPIG)*, Greifswald, Germany, 15-19 July 2014, p3-10-1.

[38]A. Fridman, Plasma Chemistry (Cambridge University Press, New York, 2008) p.620.

[39]E. M. Liston, L. Martinu, and M. R. Wertheimer, J. Adhesion Sci. Technol. **7**, 1091-1127 (1993).

[40]A-P. Herrendorf, V. Sushkov, and R. Hippler, J. Appl. Phys. **121**, 123303 (2017).

[41]L. Jiao, B. S. Truscott, H. Liu, M. N. R. Ashfold, and H. M, J. Appl. Phys. **121**, 013303 (2017).